Available online at www.sciencedirect.com
SCIENCE DIRECT®
Surface Science 586 (2005) 146–156
SURFACE SCIENCE
www.elsevier.com/locate/susc

Interpreting intensities in vibrational sum frequency generation (SFG) spectroscopy: CO adsorption on Pd surfaces

M. Morkel [a], H. Unterhalt [a], T. Klüner [b], G. Rupprechter [a,*], H.-J. Freund [a]

[a] *Fritz Haber Institute, Faradayweg 4-6, D-14195 Berlin, Germany*
[b] *Institute of Pure and Applied Chemistry, Carl von Ossietzky Universität Oldenburg, Carl-von-Ossietzky-Str. 9-11, D-26129 Oldenburg, Germany*

Received 9 March 2005; accepted for publication 3 May 2005
Available online 31 May 2005

Abstract

The lineshape and intensity of SFG signals of CO adsorbed on supported Pd nanoparticles and Pd(1 1 1) are analyzed. For CO/Pd(1 1 1) nearly symmetric lorentzian lineshapes were observed. Applying two different visible wavelengths for excitation, asymmetric lineshapes observed for the CO/Pd/Al_2O_3/NiAl(1 1 0) system are explained by a lower resonant and a higher non-resonant SFG signal and a change in the phase between resonant and non-resonant signals, most likely originating from an interband transition in the NiAl substrate. The relative intensity of different CO species (hollow, bridge, on-top) was modeled by DFT calculations of IR transition moments and Raman activities. While the (experimental) sensitivity of SFG towards different CO species strongly varies, the calculated IR and Raman activities are rather similar. The inability to exactly reproduce experimental SFG intensities suggests a strong coverage dependence of Raman activities or that non-linear effects occur that can currently not be properly accounted for.

Keywords: Sum frequency generation; Density functional calculations; Palladium; Clusters; Carbon monoxide; Chemisorption; Low index single crystal surfaces; Vibrations of adsorbed molecules

1. Introduction

Non-linear optical IR–vis sum frequency generation (SFG) vibrational spectroscopy is a versatile surface-specific technique that allows to acquire vibrational spectra of molecules adsorbed on metal or semiconductor surfaces, of molecules at liquid–gas, liquid–liquid and liquid–solid interfaces [1–11]. For solid–gas interfaces, the big advantage of SFG is its interface-specificity that allows to selectively probe adsorbed molecules even in the presence of a gas atmosphere of ~1 bar. Therefore, SFG is an excellent technique for in situ studies of

* Corresponding author. Tel.: +49 30 8413 4132; fax: +49 30 8413 4105.
E-mail address: rupprechter@fhi-berlin.mpg.de (G. Rupprechter).

0039-6028/$ - see front matter © 2005 Elsevier B.V. All rights reserved.
doi:10.1016/j.susc.2005.05.009

catalytic reactions on model catalysts [7,11–15]. Its major drawback is that a direct quantitative analysis of SFG vibrational spectra is typically difficult. For instance, the sensitivity of SFG towards different adsorbed species (such as hollow, bridge, and on-top bonded CO) may vary significantly [16] and in special cases some species may be hardly detected despite their significant surface concentration (e.g. bridge bonded CO on Pt(1 1 1) [17–19] and on Ni(1 1 1) at high CO coverages [2,20,21]). Furthermore, the sensitivity to a specific species (e.g. bridge bonded CO) may strongly depend on coverage, leading to a highly non-linear response.

Other vibrational techniques such as infrared reflection absorption spectroscopy (IRAS) may face similar problems [22,23]. Also for IRAS the observed absorbance does not necessarily scale with the surface concentration of an adsorbate (saturation of the signal intensity is often observed to set in at medium coverage [22]) but at least at low coverage the signal intensity can be related to the number of adsorbed molecules. For SFG, infrared transition moments as well as Raman scattering activities influence the signal which makes the interpretation more complex than for IR spectroscopy. For cases where two species were detected by IRAS (e.g. bridge and on-top CO on Pt(1 1 1)) and *only one* appeared in SFG (e.g. on-top CO) it was suggested that differences in the Raman scattering activities are responsible for this effect [7,18,20,24]. However, since the latter are generally not known a conclusive proof in favor or against this hypothesis has not been obtained yet.

Here we present a first step towards a better understanding and a more quantitative analysis of SFG spectra. CO adsorption on Pd(1 1 1) and Pd nanoparticles was examined by SFG spectroscopy and compared to polarization modulation (PM)-IRAS spectra [11,25], demonstrating the inherent differences between the two techniques. Experimental studies were complemented by density functional theory (DFT) cluster calculations providing harmonic stretching frequencies, infrared transition moments and Raman scattering activities, with Pd_{22} being the largest cluster studied. We show for the CO/Pd system that the observed variations in SFG signal intensity do not originate from differences in the Raman activities of the involved adsorbed species. It is rather their *coverage dependence* that is responsible for the strong non-linear response.

2. Methods

2.1. Experimental details

The experiments were carried out in a UHV system combined with an SFG-compatible UHV-high-pressure cell, as described previously [11,21]. Sample preparation was performed in the UHV section. Pd(1 1 1) was prepared by sequences of flashing to 1250 K, Ar^+ bombardment (700 V at 5×10^{-6} mbar, 5 μA current), annealing to 1250 K and oxidation between 1200 and 600 K in 5×10^{-7} mbar O_2, followed by a final flash to 1200 K. Its surface structure and cleanliness were confirmed by low energy electron diffraction (LEED), Auger electron spectroscopy (AES), and thermal desorption spectroscopy (TDS) of CO [26]. The preparation and characterization of Pd–Al_2O_3/NiAl(1 1 0) model catalysts was described in detail elsewhere [16,27] and is only briefly explained here. An ordered Al_2O_3 thin film (thickness around 0.5 nm) was grown on NiAl(1 1 0) by two sequences of oxidation in 10^{-5} mbar oxygen at 523 K. The atomic structure of the Al_2O_3 support was recently characterized by low-temperature (4 K) scanning tunnelling microscopy (STM) [28]. Pd (99.99%) was then deposited onto the alumina support at 90 K using an electron beam evaporator, finally producing Pd particles with a mean diameter of ~3.5 nm and a height of ~1.5 nm (by depositing a nominal Pd thickness of 0.4 nm; 4.5×10^{12} particles/cm^2) (for atomically resolved STM images of individual particles see [29]).

To carry out SFG spectroscopy, the model systems were transferred under UHV into the SFG cell (equipped with CaF_2 windows) which allows experiments to be carried out under UHV *as well as* pressures up to 1 bar [11,21]. CO (purity ⩾99.997%) was passed over a carbonyl absorber cartridge and introduced via a cold trap filled with liquid nitrogen (ensuring the removal of Ni- and Fe-carbonyl impurities) [15]. To produce a

well-ordered (2 × 2)-3CO structure, Pd(1 1 1) was cooled in 10^{-6} mbar CO from 300 to 100 K [15].

The laser setup consisted of a 50 Hz Nd:YAG laser (1064 nm, 30 mJ/pulse, 20 ps), followed by an SHG (second harmonic generation) unit to produce 532 nm visible light and an OPG/DFG (optical parametric generation/difference frequency generation) unit, which provided the tunable IR-light with a resolution of ~5 cm^{-1}. Pulse energies applied during the experiments were ~200 μJ for the visible and ~50–150 μJ for the IR-light (3–6 μm), at incidence angles of 50° and 55°, respectively. After passing spatial filters (apertures) and spectral (edge) filters, the generated SFG-light was detected by a photomultiplier. Every datapoint represents an average of 400 laser shots and was normalized to the incident IR- and vis-energies. Part of the SFG spectra of CO on Pd nanoparticles were acquired with another laser system based on an amplified titanium sapphire laser. About 90% of the output radiation (790 nm, 2 mJ/pulse, 2 ps, 500 Hz) was used to generate tunable infrared light (3–6 μm, ≈10 μJ/pulse) with an OPG/OPA/DFG (resolution ~25 cm^{-1}). All experiments were made in (p, p, p) polarization combination. For details on the optical setup we refer to [16,21]. PM-IRAS spectra were acquired in a second similar UHV system, equipped with a UHV-high pressure cell optimized for grazing incidence [11,25]. Spectra discussed below were taken under UHV. The method itself and high pressure (~150 mbar) PM-IRAS spectra were described elsewhere [11,25].

2.2. Computational details

All cluster calculations reported in this letter were performed on the density functional level of theory (DFT) using the B3LYP functional for exchange and correlation. Different cluster sizes were investigated, with the largest cluster containing 22 Pd atoms within a fixed geometry corresponding to Pd bulk (cf. Fig. 4). All Pd core electrons were replaced by effective core potentials (ECPs) [30], and for an accurate description of the valence electrons, a double-zeta basis set turned out to be sufficient.[1]

[1] Pd: 3s3p3d/2s2s2d from [30]; C,O: 6-31G*.

A full geometry optimization of the CO-molecule was performed for different adsorption sites (fcc/hcp threefold hollow, bridge and on-top). Furthermore, harmonic frequencies, infrared intensities and Raman scattering activities were calculated as implemented in Gaussian 98 [31]. Calculations with larger basis sets and a higher level of theory were carried out on the CO-molecule in gas phase to estimate the systematic error introduced by the limited basis sets and the approximate exchange correlation functional used.

3. Results

In this section, results on CO adsorption on Pd(1 1 1) and $Pd/Al_2O_3/NiAl(1\,1\,0)$ model catalysts are presented. We focus on the spectral intensities and the different lineshapes observed for the two systems while the assignment of the observed bands to hollow, bridge and on-top CO was already discussed in detail in previous articles [15,16,26,32]. For completeness, a brief account of SFG theory is included.

3.1. SFG-theory

For a comprehensive description of SFG theory we refer to [1,33–36] and references therein. Briefly, picosecond laser pulses at a tunable infrared frequency ω_{IR} and at a fixed visible frequency ω_{VIS} are spatially and temporally overlapped on the sample surface. Due to a second-order non-linear optical process a sum frequency signal ($\omega_{SFG} = \omega_{IR} + \omega_{vis}$) is generated. This process is considerably enhanced when the IR frequency coincides with an adsorbate vibrational resonance. Plotting the SFG signal vs. the IR wave number thus yields a vibrational spectrum. The intensity I of the generated sum-frequency signal is proportional to the incident vis- and IR-intensitites as well as the absolute square of the *effective* second-order surface susceptibility $\chi^{(2)}_{eff}$ [35].

$$I_{SFG} \propto |\chi^{(2)}_{eff}|^2 I_{IR} I_{vis} \quad (1)$$

$\chi^{(2)}_{eff}$ is defined as $\Sigma_{ijk}\{F_{ijk}\chi^{(2)}_{ijk}\}$, $\chi^{(2)}_{ijk}$ being the independent elements of the surface non-linear susceptibility $\chi^{\leftrightarrow(2)}_{s}$ and F_{ijk} are coupling factors

comprising the (linear) optical properties of the interface (i.e. the refractive indices of the involved media) and the experimental geometry (i.e. the polarizations and incidence angles), for details see [37]. However, since the interface optical properties can be considered the same for the different kinds of adsorbed CO species, the coupling factors are not included in the discussion below.

The second-order surface susceptibility $\chi_s^{(2)}$ comprises various factors, which can be separated in two parts. One part arises from the symmetry break on the surface, in the following called non-resonant background $\chi_{NR}^{(2)}$, while the other *resonant* part $\chi_R^{(2)}$ arises from the adsorbed molecules and can be described as a sum over all vibrational modes q [38].

$$\chi_s^{(2)} = \chi_{NR}^{(2)} + \chi_R^{(2)} = A_{NR} \cdot e^{i\phi_0} + \sum_q \frac{A_q \cdot e^{i\phi_q}}{(\omega_q - \omega_{IR}) - i\Gamma_q} \tag{2}$$

A_{NR}, A_q, ω_q, Γ_q and ω_{IR} refer to the non-resonant and resonant amplitude (oscillator strength), the resonance frequency, damping constant (homogeneous linewidth $2\Gamma_q$ = FWHM) of the qth vibrationally resonant mode and the infrared frequency, respectively. Both parts (amplitudes) are complex with phase factors ϕ_0 and ϕ_q and interference between them may lead to asymmetric lineshapes, as discussed in the next section. $\chi_{NR}^{(2)}$ is typically modeled by a constant complex amplitude A_{NR} because the applied light frequencies are usually far from resonances of the surface and the non-resonant background is thus independent of the IR frequency. Moreover, A_q is proportional to the dynamic dipole moment (μ_q) (determining the signal intensity in IR spectroscopy) and to the Raman scattering activity (α_q) (determining the signal intensity in Raman spectroscopy), as well as to the surface density of the adsorbate (N) and the relative amount of population of the vibrational ground state ($\Delta\rho$, which nearly equals one for CO on Pd at the temperatures studied.

$$A_q \propto N\mu_q\alpha_q\Delta\rho \tag{3}$$

Due to Eqs. (1)–(3) only vibrational modes which are *both* IR- and Raman-active are detected by SFG spectroscopy. Consequently, SFG is only allowed in a medium without inversion symmetry, i.e. the signal is generated by the adsorbate/Pd interface, while the isotropic gas phase gives no signal.

For the SFG lineshape only the *phase difference* between the non-resonant and the resonant part ($\Delta\phi_{0q}$) is important and the overall SFG intensity can thus be written as

$$I_{SFG} \propto \left| A_{NR} + \sum_q \frac{A_q \cdot e^{i\Delta\phi_{0q}}}{(\omega_q - \omega_{IR}) - i\Gamma_q} \right|^2 \cdot I_{vis} \cdot I_{IR} \tag{4}$$

which can be transformed into a expression without complex terms (assuming the same phase difference to the non-resonant background for all resonances):

$$I_{SFG} \propto A_{NR}^2 + \sum_{q=1}^{q_{max}} \left(\frac{A_q^2}{(\omega_q - \omega_{IR})^2 + \Gamma_q^2} + 2 \cdot A_{NR} A_q \cdot \frac{\Gamma_q \cdot \sin(\Delta\phi_{0q}) + (\omega_q - \omega_{IR}) \cdot \cos(\Delta\phi_{0q})}{(\omega_q - \omega_{IR})^2 + \Gamma_q^2} + \sum_{r>q}^{q_{max}} \frac{2A_q A_r \cdot (\Gamma_q\Gamma_r + (\omega_q - \omega_{IR})(\omega_r - \omega_{IR}))}{((\omega_q - \omega_{IR})^2 + \Gamma_q^2) \cdot ((\omega_r - \omega_{IR})^2 + \Gamma_r^2)} \right) \tag{5}$$

Four terms can be identified in Eq. (5). The non-resonant background, the (lorentzian) resonances, the interferences between the resonances and the non-resonant background (which is responsible for the asymmetry of the lines), and the interferences between the resonances themselves. The experimental SFG data points were fitted according to Eq. (5) to accurately extract amplitudes, resonance positions and linewidths.

3.2. Lineshapes

Vibrational modes of adsorbed molecules are usually identified by an increase of the total SFG intensity at the resonance frequency. For instance, nearly symmetric lineshapes were observed for CO or NO adsorbed on transition metal surfaces [10,11,17,39–41]. Since the resonance frequency coincides with the peak maximum it can be

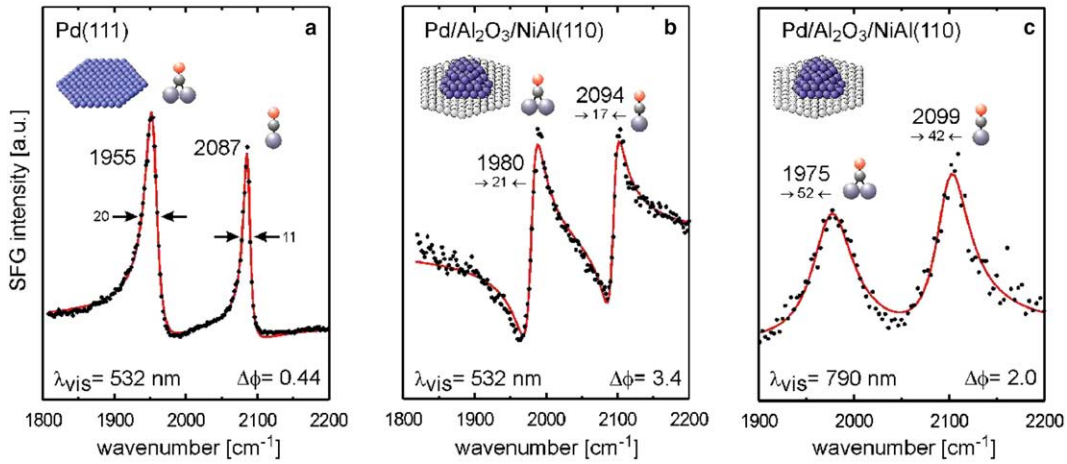

Fig. 1. SFG spectra of CO adsorption on (a) Pd(1 1 1) and (b) Pd–Al_2O_3/NiAl(1 1 0), acquired with a visible wavelength of 532 nm. (c) shows an SFG spectrum of CO adsorption on Pd–Al_2O_3/NiAl(1 1 0), acquired with visible light of 790 nm. All spectra were recorded for a CO saturation coverage at 190 K and for a mean Pd particle size of 3.5 nm.

determined by a simple ''analysis'', which also holds for the linewidth (cf. SFG spectrum of on-top and bridge bonded CO on Pd(1 1 1) in Fig. 1a). However, as apparent from Eq. (5) strongly asymmetric lineshapes and even a *signal decrease* may also occur at the resonance frequency, as previously observed e.g. for –CN or self-assembled monolayers (SAMs) on Au substrates [9,36,42–44].

A clear variation in lineshape is observed when SFG spectra of CO adsorbed on Pd(1 1 1) (Fig. 1a) and on Pd nanoparticles supported by Al_2O_3/NiAl(1 1 0) (Fig. 1b) are compared. Although CO is basically adsorbed on the same transition metal (Pd), strong asymmetric lineshapes are observed for the Pd/Al_2O_3/NiAl(1 1 0) system [45], which prevent a direct (''manual'') extraction of the relevant spectral parameters. However, all parameters (peak position, amplitude and linewidth) can be determined by applying a fitting procedure according to Eq. (5) whereby the phase difference of all resonances to the non-resonant background is fixed at the same value.

The lineshape of an SFG-resonance is primarily determined by the phase-difference $\Delta\phi_{0q}$ between the resonant and non-resonant signal. However, another condition must be fulfilled in order to obtain strong asymmetric lineshapes or even signal-dips: The non-resonant part must be *comparable or even higher* in amplitude than the resonant part, otherwise the spectra exhibit only more or less symmetric lorentzian-like peaks. In the following, the reasons for the observation of different lineshapes for the Pd(1 1 1) and Pd/Al_2O_3/NiAl(1 1 0) system are discussed, considering the two essential conditions mentioned above.

First, on the Pd/Al_2O_3/NiAl(1 1 0) sample the total amount of exposed Pd surface atoms (per cm^2 sample area) is ~70% of the corresponding value for the Pd(1 1 1) single crystal surface (1.5×10^{15} Pd atoms/cm^2 for Pd(1 1 1)). Consequently, although the *local* CO coverage on the two model catalysts is similar, the *total* amount of adsorbed CO (per sample area) is smaller on Pd/Al_2O_3 leading to a decrease of the resonant part (amplitude) of the spectrum. If (some) CO molecules on the Pd particles are tilted with respect to the NiAl substrate, the resonant signal will be further reduced, according to the metal surface selection rule [22,23]. Furthermore, the non-resonant background for the Pd/Al_2O_3/NiAl(1 1 0) system is higher than on Pd(1 1 1). SFG measurements in the absence of CO indicated that A_{NR} amounts ~50% of the (maximum) resonant CO amplitude for Pd particles and ~5% for Pd(1 1 1) (the reason for this behavior will be discussed below). As a result, the magnitudes of the resonant and non-resonant

contributions are comparable for CO/Pd/Al_2O_3/NiAl(1 1 0), which is a prerequisite for strong interference effects. Second, compared to Pd(1 1 1), also the phase difference $\Delta\phi_{0q}$ was changed significantly for Pd/Al_2O_3/NiAl(1 1 0) yielding an asymmetric SFG lineshape.

The exact origin of the phase change is not easy to identify. Since a major influence of the Pd metal can be neglected (no size- or plasmon-effects can be detected; clusters are rather large: ~3.5 nm (≈700 atoms) with an electronic structure identical to bulk Pd [27]), contributions of the Al_2O_3/NiAl(1 1 0) substrate are made responsible for the altered phase difference and, thus, altered lineshape. This suggestion is supported by measurements on the identical CO–Pd/Al_2O_3/NiAl(1 1 0) system using another SFG spectrometer, which provides a different visible wavelength (Fig. 1c [16,46]). The different excitation wavelength of 790 nm lead to a different phase relation and produced rather symmetric lineshapes (the increase in linewidth is due to the lower resolution of the OPG used for these spectra). Similar changes in lineshape upon variation of the excitation vis-wavelength were previously reported e.g. for octadecanethiol [47] and biphenyl-3-methylenethiol [44] on gold surfaces, respectively, and attributed to the excitation of electronic s–d interband transitions in the Au substrate.

As mentioned, varying the vis-energy should mainly affect the Al_2O_3/NiAl(1 1 0) substrate. Due to the very large band gap of Al_2O_3 (~8 eV [48]) an electronic excitation mechanism is probably not involved and the refractive index of alumina is therefore considered constant in the range of the applied vis energies. However, for the NiAl(1 1 0) substrate variations in the refractive index were indeed observed in the range of 1.5–2.5 eV [49,50]. Taking into account the photon energy of the two different vis pump beams, i.e. 1.6 eV (790 nm, Ti:Sa; Fig. 1c) and 2.3 eV (532 nm, Nd:YAG; Fig. 1b), variations in the non-linear susceptibility of the non-resonant background ($\chi^{(2)}_{NR}$) must be assumed, causing the observed change in lineshape [45]. This is corroborated by theoretical calculations by Knab and Koenig [51] who predicted an interband-transition around 532 nm. Although the exact mechanism is currently not fully understood, the interband-transition in the NiAl(1 1 0) substrate is most likely the key process responsible for the altered SFG lineshape.

The previous suggestion is supported by a number of further experiments that are only briefly mentioned here (Fig. 2). When CO was adsorbed

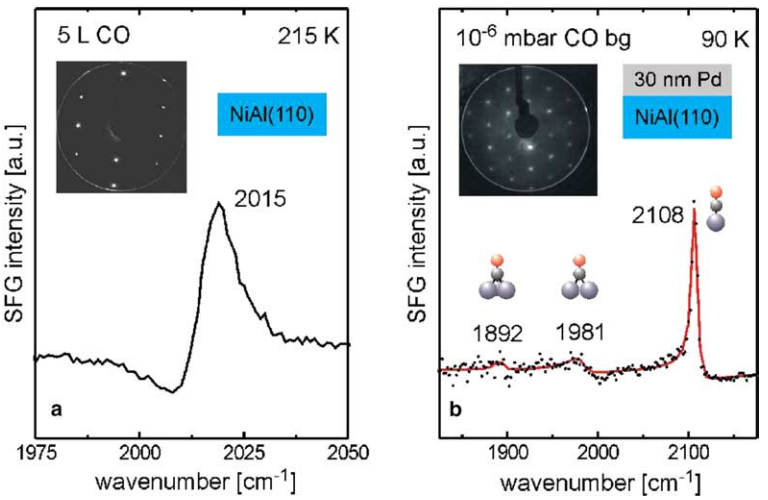

Fig. 2. SFG spectra of CO adsorption on (a) NiAl(1 1 0) and on (b) a 30 nm (1 1 1) oriented Pd film grown on NiAl(1 1 0); visible wavelength 532 nm. LEED images are shown as inset.

on NiAl(1 1 0) at 215 K a single asymmetric peak at 2015 cm^{-1} was observed (Fig. 2a; with a phase relation similar to $Pd/Al_2O_3/NiAl(1\,1\,0)$), suggesting that NiAl is in fact responsible for the lineshape (due to the large resonant signal of CO on NiAl (high CO coverage), the asymmetry is less pronounced). When a small Pd amount (0.3 nm) was deposited directly on NiAl(1 1 0) at 300 K (i.e. Al_2O_3 was absent), small Pd patches were formed on NiAl. On this sample, adsorbed CO still produced asymmetric lineshapes (similar to Fig. 1b), i.e. an effect of Al_2O_3 on the lineshape can be excluded. Finally, a 30 nm thick (1 1 1) oriented Pd film was grown on NiAl(1 1 0), i.e. the Pd film thickness was larger than the penetration depth of the visible light. Since the NiAl substrate no longer contributed to the SFG process, the phase-relation changed and rather symmetric CO adsorption bands were again observed (Fig. 2b).

It should also be pointed out that the Fano-effect is not responsible for the observed lineshape, even though the SFG lineshape of CO on Pd nanoparticles (vis wavelength 532 nm) resembles that of Fano-resonances [52,53]. A Fano-resonance originates from an interaction between a discrete excited state and an energetically degenerate continuum of states. As a result of the *coupling between these states* one observes an asymmetric lineshape due to quantum-mechanical interference effects. In a simplified picture one could consider the CO-vibration as excited state and the non-resonant background as a continuum of states, with the asymmetry being due to "some" interaction between them (e.g. dissipation of the energy into the continuum, etc.).[2] However, for the $CO/Pd/Al_2O_3/NiAl(1\,1\,0)$ system a coupling between the CO molecules and the NiAl substrate is almost impossible due to their physical separation (there are several layers of Pd and of high bandgap Al_2O_3 in between them). Due to the *absence of coupling* the observed asymmetric lineshape is not a Fano-effect but it is rather a simple optical interference phenomenon.

The different SFG lineshapes may require a more or less involved data analysis but do not represent a limitation for SFG spectroscopy in general. In contrast, limitations in the quantitative analysis somewhat reduce the impact of SFG spectroscopy and intensities are therefore discussed in detail in the following section.

3.3. Intensities

To illustrate the difficulty to relate the observed SFG signal intensity to the actual site occupation, SFG and PM-IRAS spectra of the well-known (2×2)-3CO (saturation) structure on Pd(1 1 1) are discussed in the following (Fig. 3a). The unit cell of the (2×2) superstructure contains two (fcc and hcp) hollow-bonded CO molecules and one linear-bonded CO molecule, the hollow/on-top-ratio is therefore 2:1, and the overall CO coverage is 0.75 ML. The resonance at 1898 cm^{-1} originates from threefold hollow bonded CO, while the band at 2109 cm^{-1} is assigned to linear-bonded on-top CO ([16,54] and references therein). In order to extract quantitative information, the adsorption lines of both peaks in the PM-IRAS spectrum [25] were integrated, and the SFG spectrum was fitted to derive the amplitudes (as well as exact resonance positions and linewidths). The measured hollow/on-top ratio for PM-IRAS is about 0.8:1, in agreement with previous IRAS measurements of CO/Pd(1 1 1) [55,56]. Obviously, it is (already) difficult to determine the exact site occupation from IRAS, because the absorbance does not scale with the actual coverage or site occupation. The reason for this behavior is related to different dynamic dipole moments for molecules on different adsorption sites. Furthermore, dipole-coupling effects [22] as coverage increases and "intensity borrowing" [23] can alter the signal intensity of the various species.

It is now interesting to compare the hollow/on-top ratio derived from IRAS with that of the corresponding SFG spectrum (Fig. 3a), the latter not only depending on the IR-moment but on the Raman scattering activity as well. The fitting procedure indicated a hollow/on-top (amplitude) ratio of about 0.3:1, which results in an intensity ratio

[2] In the literature different representations are used to describe Fano- and SFG-lineshapes. The Fano asymmetry is not expressed in terms of a phase factor, but is described by an asymmetry factor q [52,53]. However, the different (Fano and SFG) equations are indeed equivalent and can be transformed into each other.

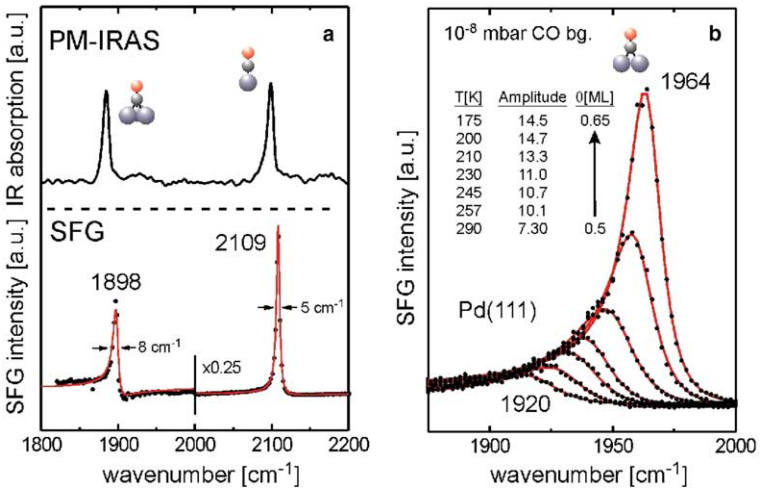

Fig. 3. (a) SFG and PM-IRAS spectra of (2×2)-3CO saturation structures on Pd(1 1 1) under UHV conditions. (b) Dependence of the SFG signal intensity of CO on Pd(1 1 1) on coverage (spectra acquired in 10^{-8} mbar CO between 290 and 175 K); visible wavelength 532 nm.

of about 0.1:1 ($I \propto |\chi^{(2)}_{\text{eff}}|^2$). Consequently, three-fold-hollow bonded CO is underestimated or, *vice versa*, on-top CO is overestimated which has already been previously reported [15,16]. For SFG, the discrepancy between measured and real site occupation may not only originate from differing IR-moments, but also from a reduced Raman scattering activity of hollow CO and/or from an increased scattering activity of linear CO. Compared to IRAS, the "overestimation" of linear-bonded CO is therefore even larger for SFG, due to the additional influence of the Raman term.

In order to provide a more fundamental basis for this discussion, DFT cluster calculations were performed. For this purpose, an isolated CO molecule was "adsorbed" on different sites of a Pd_{22} cluster (mainly exhibiting a (1 1 1) surface) and corresponding IR- and Raman-activities and singleton frequencies were calculated (Fig. 4 and Table 1). The calculated C–O stretch frequencies are in good agreement with previous calculations [32,57–59] and with experimental "singleton" (or low CO coverage) frequencies [22]. One should note that bridge and on-top bonded CO typically occur on Pd(1 1 1) only around/above 0.5 ML coverage, i.e. singleton frequencies for these species are experimentally not available (except maybe by future scanning tunnelling spectroscopy studies). The experimentally observed C–O stretch frequencies in our study are typically higher than the calculated ones, due to dynamic (dipol–dipol-coupling) and static ("via substrate", e.g. variable metal electron back-donation) effects between the CO molecules in a *high coverage* CO layer [22,23]. Such effects are, of course, absent for an isolated CO molecule. Nevertheless, the calculated carbon-metal vibrational frequencies for bridge- (388 cm^{-1}) and on-top-bonded CO (442 cm^{-1}) agree well with experimental data [60–62].

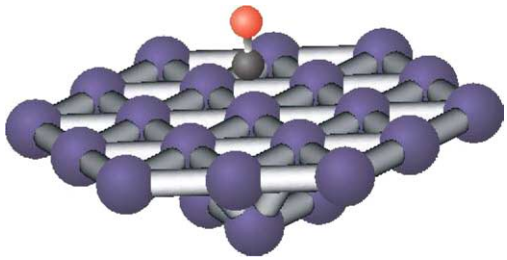

Fig. 4. Schematic model of on-top CO adsorbed on the Pd_{22} cluster, as employed for DFT calculations.

As evident from Table 1, the dynamic dipole moment is indeed somewhat (20%) *larger* for on-top bonded CO than for bridge and hollow CO, and DFT suggests a hollow/on-top ratio of about 1.4:1 for infrared spectra. However, the calculated

Table 1
Stretching frequencies, dynamic dipole moments and Raman scattering activities for isolated CO molecules on a Pd_{22} cluster exhibiting (1 1 1) facets, as calculated by density functional theory (DFT)

Binding site	Frequency [cm^{-1}]	Dynamic dipole moment μ [km/mol]	Relative IRAS-factor	Raman scattering activity [$Å^4$/mol]	Relative SFG-factor
CO_{GAS}	2209	68		12.1	–
On-top	2094*	374	1	641	1
Bridge	1891*	295	0.79	662	0.81
fcc hollow	1808*	268	0.72	697	0.78
hcp hollow	1765*	296	0.79	–	–

The frequencies marked with an (*) are corrected according to the experimental harmonic stretching frequency of molecular CO (2170 cm^{-1}) [69], i.e. the calculated values were scaled by a factor of 0.982.

higher sensitivity for on-top CO can still not explain the experimentally observed 0.8:1 hollow/on-top ratio of IRAS. As mentioned, for SFG the signal amplitudes do not only depend on the dynamic dipole moment, but also on Raman scattering activities. If one includes the calculated Raman factors (which are somewhat *smaller* for on-top CO), a hollow/on-top ratio of 1.6:1 is predicted for the (2×2) structure, which strongly differs from the experimental value of ~0.3:1. The argument of a significantly lower Raman activity of hollow bonded CO leading to a strong overestimation of on-top CO is thus not supported by the current DFT calculations. Nevertheless, according to DFT the higher sensitivity of IRAS towards on-top CO seems to be related to a higher dynamic dipole moment for linearly bonded CO.

A number of reasons may be responsible for the discrepancy between experiment and theory. The chosen cluster size should be sufficient to appropriately model CO adsorption on (1 1 1) facets. However, adsorbate–adsorbate interactions [63] are neglected in the current theoretical description, because they cannot be modeled for a cluster system within reasonable CPU-time, especially when Raman scattering activities are required. As mentioned above, coverage dependent changes as well as intensity borrowing may further complicate the situation. More complex calculations may become available in the future and are certainly required for a full analysis of signal intensities.

Fig. 3b illustrates the effect of an increasing CO coverage on the SFG signal intensity (spectra were obtained at temperatures between 290 K and 175 K in 10^{-8} mbar CO). Under these conditions, mainly bridge bonded CO was present on the surface and the CO coverage increased from about 0.5 to 0.65 ML. Fitting the spectra clearly reveals a non-proportional relationship between the CO coverage and the SFG signal amplitude. While the surface coverage increases by ~30%, the SFG amplitude doubles. One should note that the IRAS signal intensity *does not significantly change* in the same coverage regime [22,55,64]. One can therefore conclude that the strong enhancement of the SFG amplitude in Fig. 3b is rather related to coverage-dependent (increasing) Raman factors.

When SFG and IRAS spectra of CO on Pd nanoparticles are compared, a similar trend as discussed above can be observed, i.e. the SFG sensitivity is higher for on-top CO than for hollow or bridge bonded CO on (1 1 1) facets. However, for Pd nanoparticles the situation becomes much more complex due to additional contributions of CO bridge bonded to particle edges (whose intensity is strongly enhanced by "intensity borrowing" from bridge bonded CO on (1 1 1) facets [10,65]), of CO adsorbed on (1 0 0) facets and of CO bound to defect sites. Up to 8 different species (fcc and hcp hollow CO on (1 1 1) terraces, bridging CO on (1 1 1) terraces and edges and steps, on-top CO on (1 1 1) terraces and defects, bridging CO on (1 0 0) terraces) may coexist near saturation, which prevents a detailed analysis.

Based on the arguments discussed above, a direct quantitative analysis of SFG spectra is very difficult. Nevertheless, for the CO/Pd system the strong coverage-dependence of the CO stretching frequency allows to estimate surface coverages under in situ (mbar pressure) conditions. This

approach was recently confirmed by comparing (quantitative) in situ X-ray photoelectron (XPS) spectra of CO on Pd(1 1 1), acquired at mbar pressure, with corresponding SFG measurements [66]. In a similar way, thermal desorption spectroscopy (TDS) was applied under UHV conditions to relate CO coverages on Pd, Pt and Rh single crystals to the corresponding SFG spectra [26,67,68].

4. Conclusions

The lineshape and signal intensity of SFG spectra of CO adsorbed on Pd(1 1 1) and Pd/Al_2O_3/NiAl(1 1 0) model catalysts were analyzed and compared to corresponding IRAS spectra. Lineshape variations between Pd(1 1 1) and Pd/Al_2O_3/NiAl(1 1 0) could be rationalized by taking into account a possible interband-transition of NiAl when a vis-excitation radiation of 532 nm is employed. Using 790 nm vis light does not excite the interband-transition and leads to (more) symmetric lineshapes. The interpretation of SFG signal intensities remains complex since the different sensitivity of SFG towards hollow, bridge and on-top CO can not be explained by the IR and Raman moments deduced from DFT calculations. Strong coverage dependent changes of Raman moments were observed experimentally, which are currently not accessible by theoretical calculations. Provided that the SFG peak positions and, to a lesser extent, SFG intensities can be calibrated using alternative methods such as XPS or TDS, SFG spectroscopy is still a valuable tool for in situ studies of catalytic reactions.

Acknowledgments

We acknowledge support by Priority Program SPP 1091 of the German Science Foundation (project Ru 831/1-4).

References

[1] Y.R. Shen, Nature 337 (1989) 519.
[2] R.B. Hall, J.N. Russell, J. Miragliotta, P.R. Rabinowitz, in: R. Vanselow, R. Howe (Eds.), Chemistry and Physics of Solid Surfaces (Springer Series in Surface Science), vol. 22, Springer, Berlin, 1990, p. 87.
[3] K.B. Eisenthal, Chem. Rev. 96 (1996) 1343.
[4] A. Tadjeddine, A. Peremans, Surf. Sci. 368 (1996) 377.
[5] Y. Caudano, A. Peremans, P.A. Thiry, P. Dumas, A. Tadjeddine, Surf. Sci. 368 (1996) 337.
[6] G.L. Richmond, Anal. Chem. 69 (1997) 536.
[7] G.A. Somorjai, G. Rupprechter, J. Phys. Chem. B 103 (1999) 1623.
[8] R. Braun, B.D. Casson, C.D. Bain, E.W.M. van der Ham, Q.H.F. Vrehen, E.R. Eliel, A.M. Briggs, P.B. Davies, J. Chem. Phys. 110 (1999) 4634.
[9] M. Buck, M. Himmelhaus, J. Vac. Sci. Technol. A 19 (2001) 2717.
[10] G. Rupprechter, Phys. Chem. Chem. Phys. 3 (2001) 4621.
[11] G. Rupprechter, Annu. Rep. Prog. Chem., Sect. C 100 (2004) 237.
[12] P.S. Cremer, B.J. McIntyre, M. Salmeron, Y.R. Shen, G.A. Somorjai, Catal. Lett. 34 (1995) 11.
[13] G.A. Somorjai, K.R. McCrea, Adv. Catal. 45 (2000) 385.
[14] H.-R. Volpp, J. Wolfrum, in: K. Kohse-Höinghaus, J.B. Jeffries (Eds.), Applied Combustion Diagnostics, Taylor & Francis, New York, 2001.
[15] G. Rupprechter, H. Unterhalt, M. Morkel, P. Galletto, L. Hu, H.-J. Freund, Surf. Sci. 502–503 (2002) 109.
[16] H. Unterhalt, G. Rupprechter, H.-J. Freund, J. Phys. Chem. B. 106 (2002) 356.
[17] C. Klünker, M. Balden, S. Lehwald, W. Daum, Surf. Sci. 360 (1996) 104.
[18] X. Su, P.S. Cremer, Y.R. Shen, G.A. Somorjai, Phys. Rev. Lett. 77 (1996) 3858.
[19] G. Rupprechter, T. Dellwig, H. Unterhalt, H.-J. Freund, J. Phys. Chem. B 105 (2001) 3797.
[20] A. Bandara, S. Dobashi, J. Kubota, K. Onda, A. Wada, K. Domen, C. Hirose, S. Kano, Surf. Sci. 387 (1997) 312.
[21] G. Rupprechter, T. Dellwig, H. Unterhalt, H.-J. Freund, Top. Catal. 15 (2001) 19.
[22] F.M. Hoffmann, Surf. Sci. Rep. 3 (1983) 103.
[23] P. Hollins, Surf. Sci. Rep. 16 (1992) 51.
[24] H. Härle, K. Mendel, U. Metka, H.R. Volpp, L. Willms, J. Wolfrum, Chem. Phys. Lett. 279 (1997) 275.
[25] O. Rodríguez de la Fuente, M. Borasio, P. Galletto, G. Rupprechter, H.-J. Freund, Surf. Sci. 566–568 (2004) 740.
[26] M. Morkel, G. Rupprechter, H.-J. Freund, J. Chem. Phys. 119 (2003) 10853.
[27] M. Bäumer, H.-J. Freund, Prog. Surf. Sci. 61 (1999) 127.
[28] M. Kulawik, N. Nilius, H.-P. Rust, H.-J. Freund, Phys. Rev. Lett. 91 (2003) 256101.
[29] K.H. Hansen, T. Worren, S. Stempel, E. Lægsgaard, M. Bäumer, H.-J. Freund, F. Besenbacher, I. Stensgaard, Phys. Rev. Lett. 83 (1999) 4120.
[30] P.J. Hay, W.R. Wadt, J. Chem. Phys. 82 (1985) 270.
[31] M.J. Frisch et al., Gaussian 98, Revision A.7, Gaussian, Inc., Pittsburgh, PA, 1998.
[32] G. Rupprechter, M. Morkel, H.-J. Freund, R. Hirschl, Surf. Sci. 554 (2004) 43.

[33] Y.R. Shen, The Principles of Nonlinear Optics, John Wiley Inc., New York, 1984.
[34] Y.R. Shen, Annu. Rev. Phys. Chem. 40 (1989) 327.
[35] Y.R. Shen, Surf. Sci. 299/300 (1994) 551.
[36] A. Tadjeddine, Surf. Rev. Lett. 7 (2000) 423.
[37] P. Galletto, H. Unterhalt, G. Rupprechter, Chem. Phys. Lett. 367 (2003) 785.
[38] J.H. Hunt, P. Guyot-Sionnest, Y.R. Shen, Chem. Phys. Lett. 133 (1987) 189.
[39] X. Su, P.S. Cremer, Y.R. Shen, G.A. Somorjai, J. Am. Chem. Soc. 119 (1997) 3994.
[40] U. Metka, M.G. Schweitzer, H.R. Volpp, J. Wolfrum, J. Warnatz, Z. Phys. Chem. 214 (2000) 865.
[41] J.P.R. Symonds, H. Arnolds, V.L. Zhang, K. Fukutani, D.A. King, J. Chem. Phys. 120 (2004) 7158.
[42] B.S. Mendoza, W.L. Mochán, J.A. Maytorena, Phys. Rev. B 60 (1999) 14334.
[43] A. Tadjeddine, A. Le Rille, O. Pluchery, F. Vidal, W.Q. Zheng, A. Peremans, Phys. Status Solidi (a) 175 (1999) 89.
[44] C. Humbert, L. Dreesen, A.A. Mani, Y. Caudano, J.-J. Lemaire, P.A. Thiery, A. Peremans, Surf. Sci. 502–503 (2002) 203.
[45] H. Unterhalt, Ph.D. thesis, Free University Berlin, 2002.
[46] T. Dellwig, G. Rupprechter, H. Unterhalt, H.-J. Freund, Phys. Rev. Lett. 85 (2000) 776.
[47] E.A. Potterton, C.D. Bain, J. Electroanal. Chem. 409 (1996) 109.
[48] R. Jaeger, J. Libuda, M. Bäumer, K. Homann, H. Kuhlenbeck, H.-J. Freund, J. Electron Spectrosc. Relat. Phenom. 64/65 (1993) 217.
[49] K. Schlemper, PhD thesis, Technical University, Berlin, 1991.
[50] H. Jacobi, R.Z. Stahl, Metallkunde 60 (1969) 106.
[51] D. Knab, C. Koenig, J. Phys.: Condens. Matter 2 (1990) 465.
[52] U. Fano, Phys. Rev. B 124 (1961) 1866.
[53] U. Fano, J.W. Cooper, Phys. Rev. B 137 (1965) 1364.
[54] S. Surnev, M. Sock, M.G. Ramsey, F.P. Netzer, M. Wiklund, M. Borg, J.N. Andersen, Surf. Sci. 470 (2000) 171.
[55] W.K. Kuhn, J. Szanyi, D.W. Goodman, Surf. Sci. Lett. 274 (1992) L611.
[56] E. Ozensoy, D. Meier, D. Goodman, J. Phys. Chem. B. 106 (2002) 9367.
[57] K. Honkala, P. Pirila, K. Laasonen, Surf. Sci. 489 (2001) 72.
[58] D. Loffreda, D. Simon, P. Sautet, Surf. Sci. 425 (1999) 68.
[59] R. Hirschl, J. Hafner, Surf. Sci. 498 (2002) 37.
[60] R. Gómez, J.M. Pérez, J. Solla-Gullón, V. Montiel, A. Aldaz, J. Phys. Chem. B 108 (2004) 9943.
[61] C.T. Williams, A.A. Tolia, H.Y. Chan, C.G. Takoudis, M.J. Weaver, J. Catal. 163 (1996) 63.
[62] S. Park, P. Yang, P. Corredor, M.J. Weaver, J. Am. Chem. Soc. 124 (2002) 2428.
[63] A. Eichler, Surf. Sci. 526 (2003) 332.
[64] M. Tüshaus, W. Berndt, H. Conrad, A.M. Bradshaw, B. Persson, Appl. Phys. A 51 (1990) 91.
[65] K. Wolter, O. Seiferth, H. Kuhlenbeck, M. Bäumer, H.-J. Freund, Surf. Sci. 399 (1998) 190.
[66] V.V. Kaichev, I.P. Prosvirin, V.I. Bukhtiyarov, H. Unterhalt, G. Rupprechter, H.-J. Freund, J. Phys. Chem. B 107 (2003) 3522.
[67] H. Härle, A. Lehnert, U. Metka, H.-R. Volpp, L. Willms, J. Wolfrum, Appl. Phys. B 68 (1999) 567.
[68] T. Pery, M.G. Schweitzer, H.-R. Volpp, J. Wolfrum, L. Ciossu, O. Deutschmann, J. Warnatz, Proc. of the Combustion Institute, vol. 29, The Combustion Institute, 2002, p. 973.
[69] K.P. Huber, G. Herzberg, in: Molecular Spectra and Molecular Structure IV, R. Van Nostrand, New York, 1979.